REPORT DOCUMENTATION PAGE

Form Approved
OMB No. 0704-0188

1. REPORT DATE *(DD-MM-YYYY)*	2. REPORT TYPE	3. DATES COVERED *(From - To)*
10-17-2014	Interim Research Performance Report	10/24/13-10/23/14

4. TITLE AND SUBTITLE
Low-Absorption Liquid Crystals for Infrared Beam Steering

5a. CONTRACT NUMBER

5b. GRANT NUMBER
N00014-13-1-0096

5c. PROGRAM ELEMENT NUMBER

6. AUTHOR(S)
Dr. Shin-Tson Wu

5d. PROJECT NUMBER

5e. TASK NUMBER

5f. WORK UNIT NUMBER

7. PERFORMING ORGANIZATION NAME(S) AND ADDRESS(ES)
University of Central Florida
12201 Research Parkway, suite 501
Orlando, FL 32826-3246

8. PERFORMING ORGANIZATION REPORT NUMBER

9. SPONSORING/MONITORING AGENCY NAME(S) AND ADDRESS(ES)
Office of Naval Research
875 North Randolph Street
Arlington, VA 22203-1995

10. SPONSOR/MONITOR'S ACRONYM(S)
ONR 312

11. SPONSOR/MONITOR'S REPORT NUMBER(S)

12. DISTRIBUTION/AVAILABILITY STATEMENT
Approved for Public Release; Distribution is Unlimited

13. SUPPLEMENTARY NOTES

14. ABSTRACT
The objective of this project is to develop high birefringence (n), large dielectric anisotropy (), and low-loss polar nematic liquid crystal compounds and mixtures for infrared applications, especially in the MWIR spectral region. The performance goals are: n~0.2 (at ~4 m), ~5 (at 1 kHz), and absorption coefficient ≤ 5/cm.

15. SUBJECT TERMS
Low absorption, MWIR, chlorinated liquid crystals, fluorination, FTIR, eutectic mixture, deuteration, nematic phase, birefringence, overtone, fundamental mode, combination

16. SECURITY CLASSIFICATION OF:			17. LIMITATION OF ABSTRACT	18. NUMBER OF PAGES	19a. NAME OF RESPONSIBLE PERSON
a. REPORT	b. ABSTRACT	c. THIS PAGE		18	Vicky Ortiz
					19b. TELEPHONE NUMBER *(Include area code)* 407-823-6825

University of Central Florida

CREOL, The College of Optics and Photonics

Title "Low-Absorption Liquid Crystals for Infrared Beam Steering"
Grant # N00014-13-1-0096
UCF Account 65016248

On behalf of Dr. Shin-Tson Wu, I am pleased to submit the attached Interim Research Performance Report with SF 298 due 10/23/14.

For technical concerns, please contact Dr. Wu directly at swu@creol.ucf.edu. For administrative concerns, please contact Arlisia Potter, Contract Manager, at apotter@creol.ucf.edu.

Thank you.

Vicky Ortiz

Vicky Ortiz, M.A.
Coordinator of Research Programs
CREOL, The College of Optics & Photonics
University of Central Florida
407-823-6825 (ph)
407-882-9013 (fax)
vsortiz@creol.ucf.edu

UCF 50 1963–2013 50 YEARS

Enclosure: Interim Report and SF 298

CC Via email: Peter Craig, ONR
Elizabth Ford, ONR
CC Via Fed Ex: Defense Technical Information Center
ONR Regional Admin Atlanta – N66020
Naval Research Laboratory Code 5596

ONR Interim Report

Low-absorption liquid crystals for infrared beam steering

UCF Account Number: 6501-6248
ONR contract #: N00014-13-1-0096

Prepared for:	**ONR Program Manager** **Dr. Peter Criag** **Email: peter.craig@navy.mil**
Contract Period:	**Oct. 23, 2012 to Sept. 30, 2015**
Performance Period:	**Oct. 23, 2013 to Oct. 22, 2014**
Principal Investigator:	**Prof. Shin-Tson Wu** **College of Optics and Photonics** **University of Central Florida** **Orlando, Florida 32816-2700** **Email: swu@ucf.edu** **Tel: 407-823-4763** **Fax: 407-823-6880**

Abstract:

The objective of this project is to develop high birefringence (Δn), large dielectric anisotropy ($\Delta\varepsilon$), and low-loss polar nematic liquid crystal compounds and mixtures for infrared applications. To suppress IR absorption, several approaches have been investigated: 1) Shifting the absorption bands outside the spectral region of interest by deuteration, fluorination and chlorination; 2) Employing thin cell gap by choosing a high birefringence liquid crystal mixture. First, we synthesized several chlorinated terphenyls and made a eutectic mixture showing a low absorption window in the region of 4-5μm. Besides, it also possesses other attractive physical properties, such as high birefringence (Δn~0.18 at MWIR region), modest positive dielectric anisotropy ($\Delta\varepsilon$~7.82) and broad nematic temperature range. On the other hand, we formulated a high birefringence LC mixture and its birefringence is 0.26 at λ=4μm. The transmittance is higher than 98% in mid-wave infrared region. To achieve fast response time, we demonstrated a polymer network liquid crystal with 2π phase change at MWIR and response time is less than 4 ms.

Key words: Low absorption, MWIR, fluorination, chlorinated liquid crystals, eutectic mixture, nematic phase, high birefringence, polymer network liquid crystal, fast response time

1. Objective

The main objective of this program is to develop low-loss liquid crystals for electronic laser beam steering in the infrared region. Ideally, a single collimated beam of emissions from multiple lasers covering this broad band would be directed as a single beam with a common beam director. The major advantages of such a non-mechanical beam steering device are threefold: 1) reduction of system size-weight-and-power, 2) increasing mean-time-between-failure, and 3) reducing system complexity.

Beam steering based on liquid crystal (LC) optical phase array (OPA) has been demonstrated by Raytheon and Hughes since the 1980s. OPA has micro-radian precision, high diffraction efficiency and negligible side lobes, but its scanning angle is limited. To widen steering angle, one coarse OPA and one fine OPA are cascaded. For two-dimensional beam steering, two OPAs arranged in orthogonal directions are commonly used.

Recently, Vescent Photonics developed a new *refractive* beam steering device using a LC material as a cladding layer in a slab waveguide. The evanescent field of the fundamental waveguide mode interacts with the LC layer near the surface of the waveguide where the LC molecules are well-ordered (low loss) and experience high restoring forces (<0.5 ms response time) and large steering angle. The major challenge of Vescent's beam steering device (SEEOR) is its relatively long optical beam path. In the VIS and NIR spectral regions, most liquid crystals have negligible absorption so that the absorption loss is minimal. In the MWIR and LWIR regions, some closely overlapped molecular vibration bands exist. As a result, the baseline absorption coefficient of 5CB (cyano-biphenyl) reaches ~10 cm^{-1}. In a 2π-modulo OPA, the employed LC layer is usually thinner than 10 μm. Thus, the absorption loss is ~1%. But in Vescent's SEEOR, the optical path length could be as long as few millimeters and the absorption loss could be significant. Thus, there is an urgent need to develop low-loss liquid crystals in order to extend SEEOR operation to MWIR and LWIR.

2. Technical Approach

A major challenge for IR applications of liquid crystals is the inherently large absorption loss due to some overlapping molecular vibration bands and their overtones. In the off-resonance regions, the baseline absorption coefficient of 5CB reaches as high as α~10 cm^{-1} [ST Wu, J. Appl. Phys. 84, 4462 (1998)]. The transmittance (T) of a liquid crystal layer can be expressed as

$$T = e^{-\alpha d}, \tag{1}$$

where α is the absorption coefficient and d is the LC layer thickness. Let us take α~10 cm^{-1} as an example. For a 10-μm-thick LC layer, αd=0.01 and the transmittance remains 99%. However, if the LC layer thickness (or effective optical path length) increases, then the absorption will increase exponentially, as Eq. (1) indicates. To improve transmittance, two approaches are commonly pursued: 1) To minimize absorption coefficient α by selecting proper functional groups, while maintaining nematic phase; and 2) To reduce the cell gap d or optical path length by using a high birefringence LC material. Here we define a figure-of-merit (*FoM*) to compare the performance of an LC:

$$FoM = \frac{\Delta n}{\alpha}. \tag{2}$$

The molecular vibration frequency (ω) of a diatomic group depends on the spring constant (κ) and the effective mass (m) as:

$$\omega = \sqrt{\kappa/m}. \quad (3)$$

As the effective mass increases the vibration frequency decreases, i.e., the absorption band shifts toward a longer wavelength. Table 1 shows some common absorption bands that occur in MWIR and LWIR regions: e.g., CH stretching, CN stretching, C=C stretching in phenyl rings, C-H in-plane deformation, C-C skeletal stretching, C-F stretching, and C-H out-of-plane deformation.

Table 1: IR absorption of different functional groups in typical liquid crystals. (str.=stretching; s.=strong absorption; m.=medium absorption; def.=deformation; w.=weak absorption; v.=variable intensity) [B. D. Mistry, *A Handbook of Spectroscopic Data: Chemistry-UV, IR, PMR, CNMR and Mass Spectroscopy,* Oxford, 2009]

	Vibration mode	Frequency (cm^{-1})	Wavelength (μm)	Relative intensity
C-H in phenyl ring	str.	3095-3010	3.23-3.32	m.
$-CH_2-$, $-CH_3$	str.	2950-2845	3.39-3.51	m.
C≡N	str.	2185-2120	4.58-4.72	s.
C≡C (non terminal)	str.	2260-2190	4.42-4.57	very weak
C-H in phenyl ring	str. overtone	1850-1780	5.40-5.62	m.
C=C	str.	1625	6.16	v.
C-H in $-CH_2-$	def.	1485-1445	6.74-6.92	m.
C-H in $-CH_3$	def.	1470-1430	6.80-7.00	m.
C-H in phenyl ring	in-plane def.	1225-950	8.16-10.53	w.
C-C	skeletal str.	1300-700	7.69-14.29	m.
C-F	str.	1100-1000	9.01-10.00	s.
$-CF_2-$	str.	1250-1050	8.00-9.50	s.
$-CF_3$	str.	1400-1100	7.14-9.10	s.
C-Cl	str.	800-600	12.5-16.67	s.
C-H in phenyl ring	out-of-plane def.	900-670	11.11-14.93	w.

More specifically, in the MWIR region the following absorption bonds dominate: the C-H stretching in a phenyl ring,–CH_2– and –CH_3 stretching from an alkyl chain, C≡N stretching from the cyano polar group, and some overtones from in-plane and out-of-plane C-H deformations. On the other hand, in the LWIR region following absorption bands dominate: C-H in-plane and out-of-plane stretching, C-C skeletal stretching, and C-F stretching.

From Eq. (3), three approaches can be considered to shift the absorption bands outside the spectral region of interest: deuteration, fluorination, and chlorination.

1) Deuteration: Substituting hydrogen with deuterium doubles the effective mass. As a result, the molecular vibration frequency would shift toward a longer wavelength by a factor of $\sqrt{2}$. The C-D in-plane and out-of-plane deformations would occur outside the LWIR region. However, deuteration shifts the C-H vibration in alkyl chain (~3.5 μm) to ~4.8 μm [ST Wu, et al. J. Appl. Phys. 92, 7146 (2002)]. *Therefore, to reduce absorption for both LWIR and MWIR bands we should do deuteration only for the phenyl rings, but not for the alkyl chain.*

2) Fluorination: As shown in Table 1, the vibration frequencies of CF, CF_2 and CF_3 occur in the LWIR region. *Therefore, fluorination could be favorable for MWIR but is unfavorable for LWIR.* However, a special caution must be taken. From Table 1, the overtones of CF, CF_2 and CF_3 could appear in the MWIR region. This is indeed observed in our recent studies of fluorinated terphenyl liquid crystal in the MWIR region [Y. Chen, et al. Opt. Express 19, 10843 (2011)]. Although the overtone intensity is reduced significantly, it is still noticeable especially when the optical path length is long.

3) Chlorination: As shown in Table 1, the C-Cl vibration frequency occurs at 800-600 cm^{-1}, which is outside the LWIR band. Moreover, its overtone will not show up in the MWIR region. Therefore, from an absorption viewpoint C-Cl seems to be a better polar group than CN and CF. We have previous experiences in chlorinated liquid crystals [ST Wu, et al. Liq. Cryst. 10, 635 (1991)], but not aimed for IR applications. Here we report some new chloro LC compounds with special emphasis on low IR absorption.

On the other hand, a high birefringence LC is desirable for reducing the cell gap d or optical path length. Thinner cell gap also helps to achieve fast response time for nematic liquid crystal. The LC birefringence is governed primarily by the molecular conjugation, which is contributed by the core structure and terminal groups. Due to UV instability of double bonds and carbon-carbon triple bonds, conjugated phenyl rings have been commonly used for obtaining high birefringence. However, using too many phenyl rings will result in several drawbacks: 1) its melting point will be too high to be used at room temperature; 2) its viscosity will increase; 3) its birefringence will saturated once there are more than four phenyl rings. Therefore, terphenyl could be an optimal core structure. In terms of polar group, -F,-Cl,-NCS, -CN are commonly used in LC compounds to provide dipole moment. With the same core structure, -F and –Cl provide large resistivity and modest dipole moment. Therefore, they are widely used in the TFT-LCDs. –NCS provides large birefringence and dielectric anisotropy with keeping modest viscosity, while its properties will deteriorate after UV exposure. –CN helps increase birefringence, dielectric anisotropy and shows good UV stability, while it may result in large viscosity and response time. To achieve fast response time, polymer network liquid crystal (PNLC) is considered.

3. Progress

3.1 Benchmark 5CB

Here, we use 5CB (4'-pentylbiphenyl-4-carbonitrile) as benchmark for comparison. Figure 1 depicts the measured absorption coefficient of 5CB from 4000 cm^{-1} to 650 cm^{-1}. The measurement was conducted in an isotropic phase in order to avoid scattering and two cells with 100 μm and 50 μm gaps were employed.

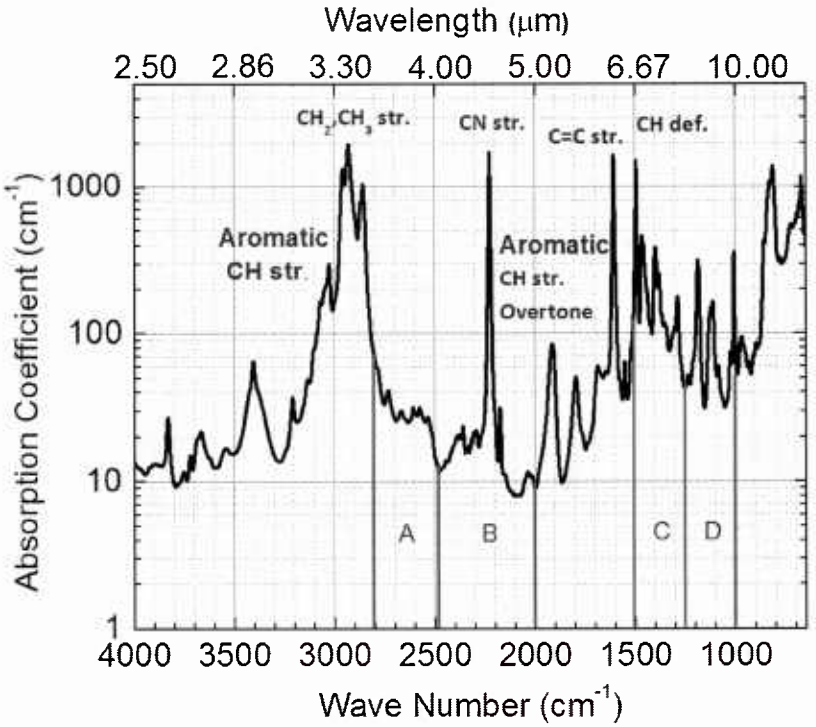

Fig.1 Measured absorption coefficient spectrum of 5CB.

From Fig. 1, the carbon-hydride stretching band (including CH_2 and CH_3) is quite broad (3300-2800 cm^{-1}) and strong, and the peak absorption coefficient exceeds 1000 cm^{-1}. In the center of MWIR (2500 cm^{-1} to 2000 cm^{-1}, marked as Zone B), the C≡N stretching shows a narrow but very strong absorption. Cyano is a strong polar group and electron acceptor; it not only provides a large dielectric anisotropy but also helps to increase birefringence. For practical applications, a large $\Delta\varepsilon$ helps to reduce operation voltage while high Δn enables a thinner LC layer to be used for reaching the required phase change. Unfortunately, CN has a strong absorption band at λ=4.45 μm, so it should be avoided because it raises the baseline absorption. A molecular vibration band usually has Lorentzian shape and its tail could spread broadly. The overlap of the neighboring bands is responsible for the observed baseline absorption.

Besides the normal vibration mode of C≡N, the baseline absorption in Zone B also comes from the overtone (doubled frequency of a given band or sum frequency of two separated bands) of the absorption bands in Zone D, as marked in Fig. 1. As listed in Table 2, the C-C (in the alkyl chain) skeletal stretching (1300-700 cm^{-1}) and the in-plane deformation of C-H in the phenyl rings (1225-950 cm^{-1}) contribute to the absorption in Zone D. The absorption of Zone C consists of the C-H (in alkyl chain) deformation and C-C skeletal stretching, whose overtone further increases the baseline absorption observed in Zone A. The tail of the absorption band in Zone A may also raise the absorption level in Zone B. Therefore, the absorption in Zones A and B are primarily influenced by four mechanisms: 1) strong CN stretching, 2) absorption tail from the CH stretching of the alkyl chain, 3) absorption tail from the overtone CH stretching of the phenyl ring, and 4) the overtone absorption from Zones C and D.

Table 2: Possible absorption mechanisms for Zones A-D shown in Fig. 1.

Zone	Absorption Mechanism	Frequency (cm^{-1})	Wavelength (μm)
A	C-H (in CH_2,CH_3) def. overtone C-C skeletal str. overtone	2790-2500	3.6-5.0
B	C≡N str. C-H (in phenyl ring) in-plane def. overtone C-C (in alkyl chain) skeletal str. overtone	2000-2500	4.0-5.0
C	C-H (in CH_2, CH_3) def. C-C skeletal str.	1485-1250	6.7-8.0
D	C-H (in phenyl ring) in-plane def. C-C (in alkyl chain) skeletal str.	1000-1250	8.0-10.0

Based on above mentioned analyses, we outline the following molecular design strategies to suppress the absorption in Zone B (2500-2000 cm^{-1}). Some basic structure elements cannot be removed as they are required to maintain mesogenic phase. The key is to reduce the transition intensity and overlap from these fundamental frequencies and their overtones. The latter is critically important but is often unpredictable.

A. Polar group

We should avoid using C≡N or NCS, instead we propose to employ C-F or C-Cl as polar groups. The C-F bond shows absorption in the 1400-1100 cm^{-1} range. Its overtone may occur at 2200-2000 cm^{-1}, but it is fairly weak. On the other hand, the absorption band for C-Cl bond is in the range of 800-600 cm^{-1}, and the second-harmonic overtone should not appear in the 2500-2000 cm^{-1} range. Although C-Cl polar group is preferred in terms of absorption, its mesogenic phase is difficult to predict. We need to synthesize several chlorinated compounds and examine their LC properties.

B. Short alkyl chain

To form liquid crystal phase, a flexible side chain and certain length-to-width ratio are required. A too rigid compound usually does not exhibit a mesogenic phase. Even it does, its melting point could be too high to be practically useful. However, the longer the alkyl chain, the stronger the absorption loss in the MWIR and LWIR regions. Therefore, to suppress the overtone absorption of C-C skeletal stretching, a shorter flexible alkyl chain, e.g., C_2H_5 or C_3H_7, is preferred. Moreover, with shorter alkyl chain the C-H absorption in both stretching and deformation bands will also be reduced and the tail of CH absorption band is also suppressed. Thus, a delicate balance between absorption and mesogenic phase needs to be considered.

C. Core structure

CH bonds are found in both alkyl chains and aromatic rings. Although a cyclohexane ring helps widen the nematic range, it makes little contribution to birefringence. Therefore, to achieve high birefringence, we consider terphenyl as core structure. Moreover, the in-plane deformation of C-

H (1225-950 cm^{-1}) in the phenyl rings occurs when there are two or more adjacent CH bonds. Proper substitutions with F or Cl could avoid the coupling of two or more adjacent CH bonds and reduce the in-plane deformation absorption.

3.2 LC compounds and mixtures

Table 3: Chemical structures and properties of the eleven compounds studied, where Cr stands for crystalline, N for nematic, and I for isotropic phase.

No.	Structure	PTT(°C)
1	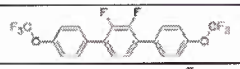	Cr 86 N 88 I
2	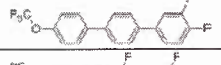	Cr 86 N (84) I[a]
3	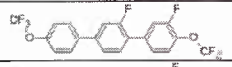	Cr 55 N (40) I
4	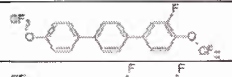	Cr 113 I
5	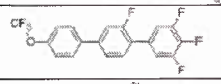	Cr 66 I
6	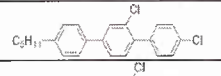	Cr 71 (N 65) I
7	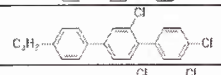	Cr 95 (N 68) I
8	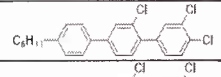	Nematic phase at room temperature
9	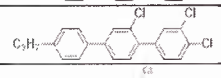	Nematic phase at room temperature
10		Cr106.29(N70.6)I
11		Cr78.3(N45)I

[a]() indicates a monotropic phase

Based on our design strategies, we prepared five fluorinated and two chlorinated terphenyl compounds as listed in Table 3. Also included are their phase transition temperature (*PTT*) and heat fusion enthalpy (ΔH). To suppress absorption, we replace all the CH bonds in the alkyl chain by $-OCF_3$, but keep the CH bonds in the phenyl rings in order to obtain nematic phase. Moreover, the CH bonds in the phenyl rings exhibit a much weaker and narrower absorption than those in the flexible alkyl chain. The phase transition temperatures were measured by Differential Scanning Calorimetry (DSC, TA instruments Q100). The first three compounds have nematic phase. To widen the nematic range, we formulated a eutectic mixture, designated as UCF-1, using these five fluoro compounds. The melting point (T_m) is 42°C and clearing point (T_c) is 51.5°C during the heating cycle. Due to super-cooling effect, UCF-1 remains liquid at room temperatures for several days.

3.2.1 Low absorption

To measure MWIR absorption, we filled UCF-1 to a LC cell with two bare barium fluoride (BaF_2) substrates and measured its transmittance using a Perkin Elmer Spectrum One FTIR Spectrometer. BaF_2 is highly transparent from UV to ~10μm. It refractive index 1.47 is close to that of LC. The cell gap was ~46μm. To eliminate scattering, we conducted the absorption

measurement at an isotropic phase (~60°C). To take surface reflections into consideration, we used a single BaF_2 as the reference. Figure 2 shows the measured absorption coefficient of UCF-1. Also included in Fig. 1 for comparison is 5CB. For UCF-1, it shows a relatively low absorption coefficient (α~2.3 cm^{-1}) in the vicinities of 3333 cm^{-1}, i.e. λ~3μm, and the absorption coefficient is smaller than 3 cm^{-1} in the region of 3571-3333 cm^{-1} (2.8~3.0 μm). Besides, the absorption at 3030-2778 cm^{-1} (3.3~3.6 μm) is significantly reduced because the alkyl chain has been replaced. The absorption peak at 3049 cm^{-1} (3.28 μm) originates from the CH vibration in the phenyl rings. It overlaps with the peak of 5CB very well. Even though the absorption peak resulting from C-O and C-F stretching vibrations are shifted to the 1302-1156 cm^{-1} (7.68~8.65μm) region, their combined overtone results in a modest (~80cm^{-1}) but broad absorption peak in the vicinities of λ=4 μm.

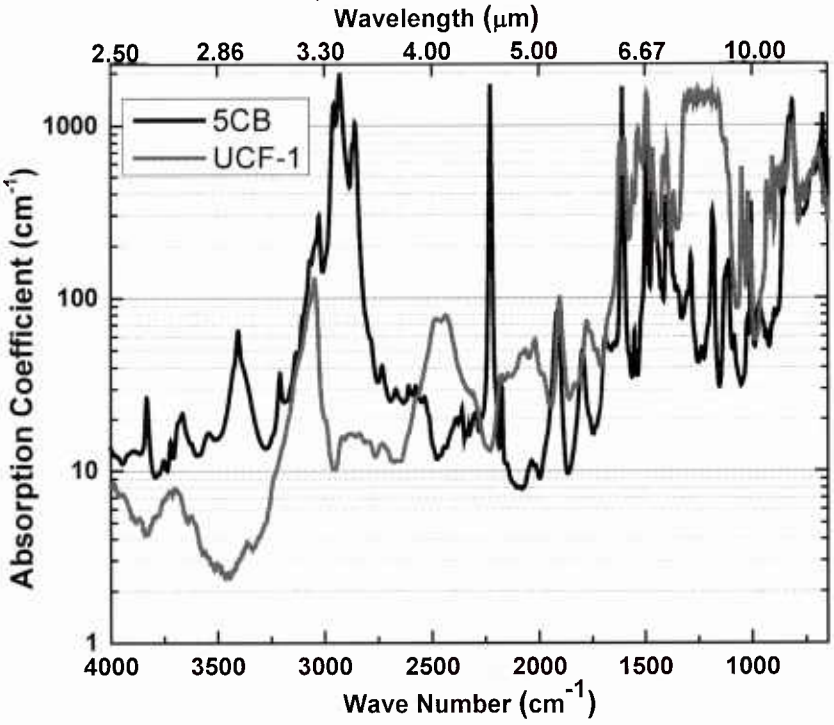

Fig. 2: Measured absorption spectrum of 5CB (black line) and UCF-1 (red line).

To shift overtone resonance peak out of MWIR, we replaced the fluorine with a heavier atom, chlorine. While, for chlorinated compounds, the alkyl chains need to be kept to maintain the flexibility and aspect ratio of the LC compounds. Otherwise, some undesirable properties, such as high melting point, large heat fusion enthalpy, and high viscosity could occur. More seriously, the compounds may not have any mesogenic phase. The physical properties of some chlorinated LCs for display applications (low birefringence) have been reported previously. Thus, here we synthesized two high birefringence chlorinated compounds (#6 and #7) listed in Table 3. Both compounds exhibit monotropic phase. We prepared a binary mixture with 60 wt% compound 6 and 40 wt% compound 7, designated as UCF-2. The nematic range of UCF-2 is from 48.3°C to 69.2°C in the heating process. Super-cooling effect lowers the melting point to ~0°C. Thus, UCF-2 remains liquid crystal phase at room temperature (~25°C). To measure the MWIR absorption spectrum, we filled UCF-2 to a BaF_2 cell with cell gap ~46μm. The measurement procedures are the same as UCF-1.

Figure 3 depicts the measured absorption spectrum of UCF-2 in the IR region. The absorption spectrum of 5CB is also included for comparison. UCF-2 exhibits a relative clean absorption in the 4000-3125cm^{-1} (2.5~3.2μm). The lowest α is 4 cm^{-1} at 3247cm^{-1} (λ=3.08μm), which is slightly higher than that of UCF-1. The responsible absorption mechanism in this region is the CH in-plane deformation. In UCF-1, more CH bonds are substituted by C-F bonds so that the in-plane vibration effect is suppressed.

More importantly, UCF-2 shows a relatively small absorption in the 2778-1923 cm^{-1} (or 3.6 μm to 5.2 μm) window. The reasons are twofold: 1) In comparison with 5CB, the CN vibration band centered at 4.45μm is removed, and 2) In comparison with UCF-1, the vibration peaks resulting from C-Cl bonds are shifted to beyond 12.5 μm, and thus the overtone is still outside the MWIR region. The strong resonance peak centered at 2941cm^{-1} (3.4 μm) is due to the CH bonds at alkyl chain. Thus, it has similar shape to the resonance peak of 5CB but with weaker amplitude, because 5CB has a longer alkyl chain than the chlorinated compound (#7). Thus, UCF-2 shows a lower absorption than 5CB in the 4-5 μm MWIR region.

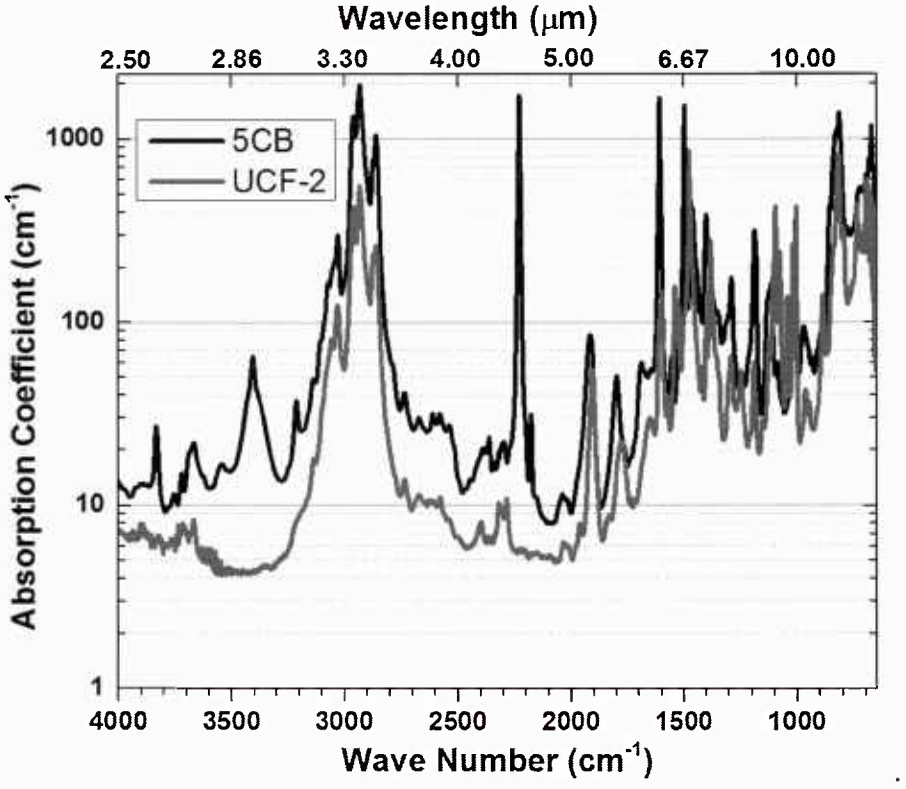

Fig. 3: Measured absorption coefficient of 5CB (black line) and UCF-2 (red line).

3.2.2 Physical properties

In addition to low absorption, the mixture is also required to have high birefringence, low viscosity and modest dielectric anisotropy. Therefore, we also characterized the physical properties of UCF-2.

A. Birefringence

Birefringence can be obtained by measuring the voltage dependent transmittance of a homogeneous cell sandwiched between two crossed polarizers. We prepared two homogeneous

cells with strong anchoring energy and cell gap d~5μm. In the visible and near IR regions, we can still use indium-tin-oxide (ITO) coated glass substrates. UCF-1 and UCF-2 were filled into the LC cells at ~70°C and 80°C, respectively. Then, both cells were mounted on a Linkam LTS 350 Large Area Heating/ Freezing Stage controlled by TMS94 Temperature Programmer. To obtain maximum transmittance, the LC director was oriented at 45° with respect to the polarizer transmission axis. A linearly polarized He-Ne laser (λ=633nm), a tunable Argon-ion laser (λ=514nm, 488nm and 457nm) and a semiconductor laser (λ=1550nm) were used as the light sources. A 1 kHz square-wave AC signal was applied to the LC cells. The transmitted light was measured by a photodiode detector and recorded by a LabVIEW data acquisition system (DAQ, PCI6110). Thus, the corresponding VT curves and phase retardation were measured. The birefringence at a given wavelength and temperature was obtained from the phase retardation based on the following equation:

$$\delta = 2\pi d\Delta n / \lambda, \tag{4}$$

here δ is the phase change, d is the cell gap, Δn is the birefringence and λ is the laser wavelength.

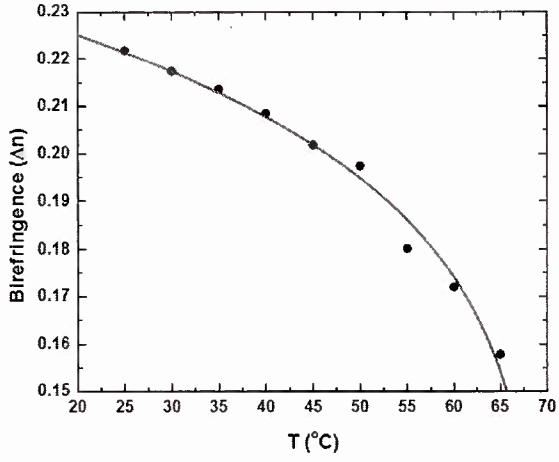

Fig. 4: Temperature dependent birefringence of UCF-2 λ=633nm: dots stand for measured data and red line for fitting curve with Eq. (5).

The temperature dependent birefringence of UCF-2 was measured from 25°C to 65°C, and the results for λ=633nm are plotted in Fig. 4, where dots are experimental data and red line is the fitting curve based on Haller's semi-empirical equation:

$$\Delta n = \Delta n_0 (1 - T/T_c)^{\beta}, \tag{5}$$

here Δn_0 is the extrapolated birefringence at T=0K and β is a material constant. Through fitting, we find Δn_0=0.303 and β=0.153.

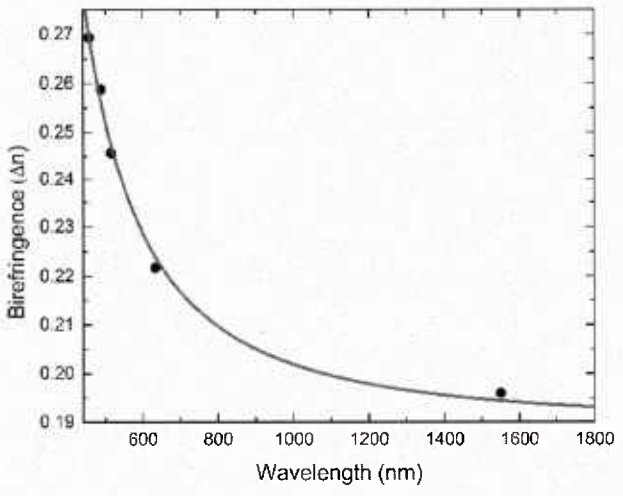

Fig. 5: Birefringence dispersion of UCF-2 at room temperature: dots are measured data and solid line is fitting with Eq. (6).

To determine the birefringence in the MWIR region, we measured the dispersion curve using several visible and short-wave IR lasers at 25°C. Results are plotted in Fig. 5. Dots are measured data at five discrete laser wavelengths and red line represents the fitting results using following single-band model:

$$\Delta n = G\frac{\lambda^2\lambda^{*2}}{\lambda^2-\lambda^{*2}}, \tag{6}$$

where G is a proportionality constant and λ^* is the mean resonance wavelength. Through fitting, we find G=3.05μm^{-2} and λ^*=0.249μm. Based on these parameters, the birefringence at any wavelength can be calculated through Eq. (6). In the MWIR region in which $\lambda>>\lambda^*$, the birefringence is decreased to a plateau, its value is about 10%~20% lower than that in the visible region. For UCF-2, the birefringence in the MWIR region is still relatively high (Δn~0.19). Higher birefringence enables a thinner cell gap to be used for achieving a certain phase change, say 2π, which in turns helps improve response time. We also measured the birefringence of UCF-1, and its Δn=0.17 at T=25°C and λ=633nm, which is much smaller than that of UCF-2 (Δn=0.22).

B. Viscosity

The visco-elastic coefficient (γ_1/K_{11}) was obtained by measuring the dynamic free relaxation time for a controlled phase change as:

$$\delta(t) = \delta_0 \exp\left(-\frac{2t}{\tau_0}\right), \tag{7}$$

$$\tau_0 = \frac{\gamma_1 d^2}{K_{11}\pi}, \tag{8}$$

here δ_0 is the total phase change, τ_0 is the relaxation time, γ_1 is rotational viscosity and K_{11} is the splay elastic constant. We plot visco-elastic coefficient for UCF-2 at different temperatures in Fig. 6, where dots are experimental data and red line is fitting curve with following equation:

$$\frac{\gamma_1}{K_{11}} = A\frac{\exp(E/K_BT)}{(1-T/T_C)}. \tag{9}$$

In Eq. (9), A is the proportionality constant, E is the activation energy, T is the Kelvin temperature and K_B is the Boltzmann constant. For UCF-2, we find $A=1.11\times10^{-7}$ ms/μm^2 and E=531meV. UCF-2 has a much larger visco-elastic coefficient (~140 ms/μm^2) than UCF-1 (~25 ms/μm^2) at room temperature. The possible explanations are: 1) the chlorine atom is heavier and bulkier than fluorine, and 2) the chloro compounds have longer alkyl chain. As the temperature increases, the visco-elastic coefficient decreases significantly.

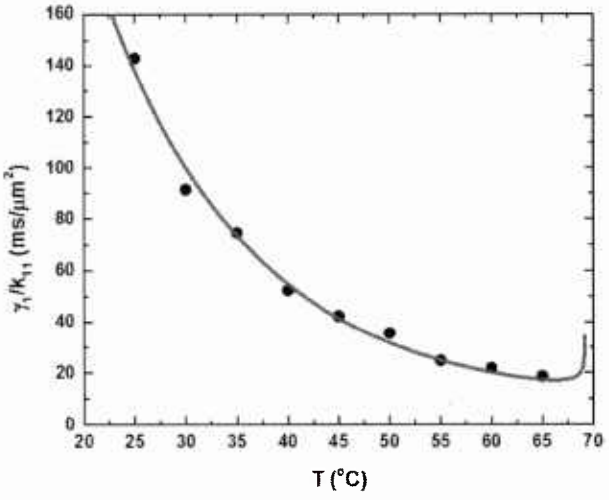

Fig. 6: Temperature dependent visco-elastic coefficient of UCF-2; dots are measured data and red line is fitting with Eq. (9). λ=633nm.

C. Dielectric anisotropy

To determine the dielectric anisotropy, we measured the capacitance of a homogenous cell and a homeotropic cell using an HP-4274 multi-frequency LCR meter. For UCF-2, $\Delta\varepsilon$=7.82 at 25°C. This medium dielectric anisotropy results from the modest C-Cl dipole group. UCF-1 aligns well in homogeneous cells, but not so well in homeotropic cells. Therefore, we can only estimate its $\Delta\varepsilon$ value through the measured threshold voltage ($3.4V_{rms}$) from a homogeneous cell. The estimated $\Delta\varepsilon$ is about 4. This small $\Delta\varepsilon$ value can be easily understood because some compounds listed in Table 2 have dipoles on both terminal groups. As a result, their dipole moments cancel each other.

3.3 High birefringence liquid crystal mixtures

First, we prepared a commercially available high birefringence LC mixture (developed by our group several years ago), which shows Δn=0.53 at λ=514nm and γ_1/K_{11}=17.0 ms/μm^2 at room temperature. By measuring its birefringence at different wavelengths, we obtained its extrapolated Δn=0.35 at λ=4μm. If we employ a cell with d=12μm in order to satisfy 2π phase change, the response time would be ~125ms. Moreover, this mixture mainly contains compounds with –NCS polar group. As a result, its absorption is quite strong in the 4.5~5.5μm region and the transmittance is only 95% at off-resonance region with d=12μm.

To avoid using NCS group, we prepared four cyano-terphenyl compounds listed in Table 4. Though –CN group has a very strong peak at ~4.45μm, the absorption band is relatively narrow. While –CN bond elongates the conjugation length of the LC molecule and hence helps to increase the birefringence. The phase sequence and heating enthalpy of different compounds

were measured using Differential Scanning Calorimeter (DSC). As shown in Table 4, these compounds have a relatively high melting point. To lower the melting point, we formulated a eutectic mixture by these four compounds. The melting point of this quaternary mixture is decreased to 36.3 °C. In order to further lower the melting point, we mixed 35 wt% UCF-2 into the cyano-terphenyl host. The resulting melting point of this mixture (UCF-3) is lower than -4°C. The clearing point is 149.7°C, which shows super broad nematic temperature range.

Table 4: Chemical structures and properties of the cyano-terphenyl compounds studied, where Cr stands for crystalline, N for nematic, and I for isotropic phase.

No.	Structure	PTT(°C)
1	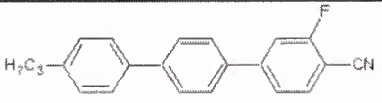	Cr 108.7 N 198.8 Iso
2	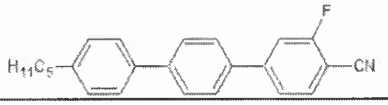	Cr 86.1 N 182.6 Iso
3	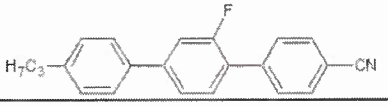	Cr 91.3 N 208.1 Iso
4	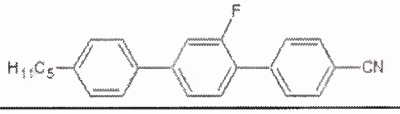	Cr 92.7 N 190.9 Iso

We also measured the electro-optic properties of UCF-3. The testing methods are the same as what we used for UCF-2. Figure 7 shows the dispersion curve of UCF-3. The red line is the fitting curve with Eq. (6): G=3.78μm^{-1} and λ^*=0.258μm. The birefringence saturates in the IR region where $\lambda >> \lambda^*$. The birefringence of UCF-3 is Δn=0.26 at λ=4μm; this high birefringence helps to reduce the required optical path length.

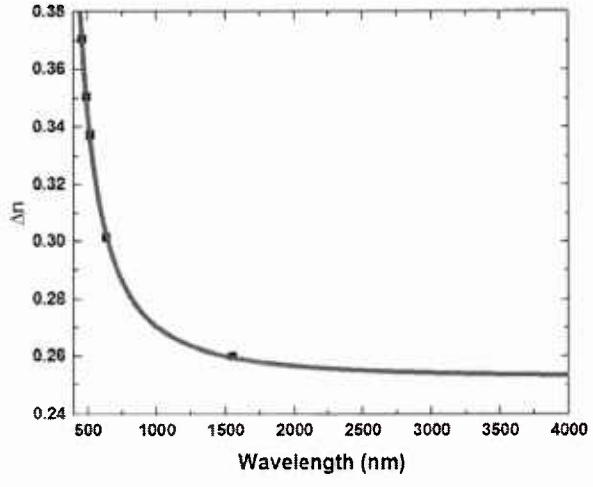

Fig. 7: Birefringence dispersion of UCF-3 at room temperature; dots are measured data and solid line is fitting with Eq. (6).

Therefore, the required cell gap for 2π phase change is 24μm at λ=4μm in transmissive mode. We fabricated a liquid crystal cell by employing two BaF_2 substrates with homogeneous rubbing. The cell gap was controlled at 24μm by spacers. The transmittance spectrum was measured by FTIR at room temperature as well. Since LC molecules are aligned well with rubbing force, light scattering caused by LC directors is negligible. Figure 8 shows the measured transmittance spectrum in the MWIR region. Although there is a strong peak at λ=4.45μm due to the –CN vibration, it shows high transmittance (T>98%) in the off-resonance region.

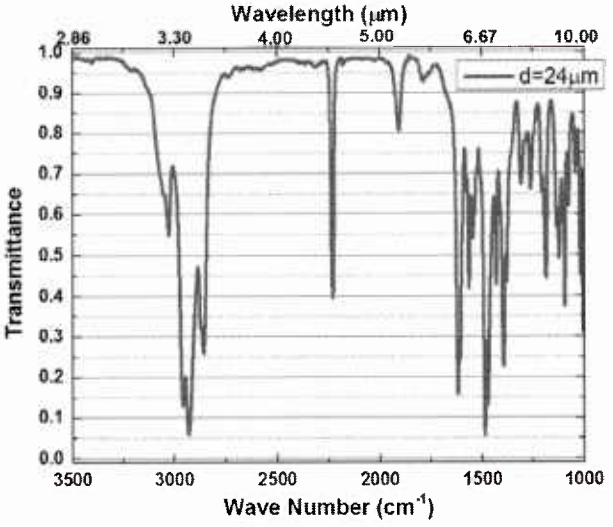

Fig. 8: Measured transmittance spectrum of UCF-3 at MWIR. Cell gap d=24μm.

Figure 9 depicts the temperature dependent visco-elastic constant of UCF-3. At room temperature (T=22°C), γ_1/K_{11}=113 ms/μm^2. The relatively large viscosity results from the rigid terphenyl cores, the cyano groups and chloro substitution. As the temperature increases, the visco-elastic constant decreases dramatically. The solid line in Fig. 9 is fitting with Eq. (9). The fitting parameters are: A=1.38x10^{-7} ms/μm^2 and E=521.4 meV. Thus, such a large viscosity results in slow response time, which is not preferred in the beam steering applications. Therefore, polymer network liquid crystal is considered for achieving fast response time.

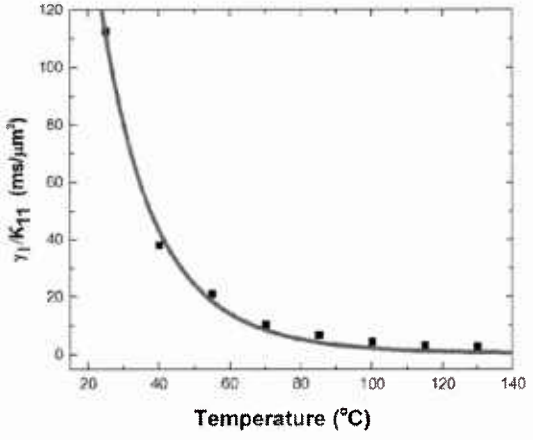

Fig. 9: Temperature dependent visco-elastic coefficient of UCF-3: dots are measured data and red line is fitting with Eq. (8). λ=633nm.

3.4 Polymer network liquid crystal (PNLC)

To fabricate PNLCs, we prepared a precursor by mixing 94.5wt% of UCF-3, with 5.0 wt% of RM257 and 0.5 wt% of photo-initiator. Here, we just used a monomer (RM257) with mesogenic phase to maintain good alignment and obtain uniform phase profile. Then, the precursor was filled into homogeneous LC cells (indium tin oxide glass substrates). The cell gap was controlled at 11.8μm and the effective optical path is ~24μm in a reflective mode, which will satisfy the 2π phase change at λ=4μm. A thin cell gap helps to reduce the operation voltage. In the UV curing process, we controlled the curing temperature at 0°C to obtain small domain size, which in turn leads to fast response time. Here, a UV LED lamp (λ=385nm, Intensity~300mW/cm^2) was employed and the exposure time for one hour. Since both terphenyl and cyano structures are stable under UV exposure, UCF-3 is a good host for PNLC.

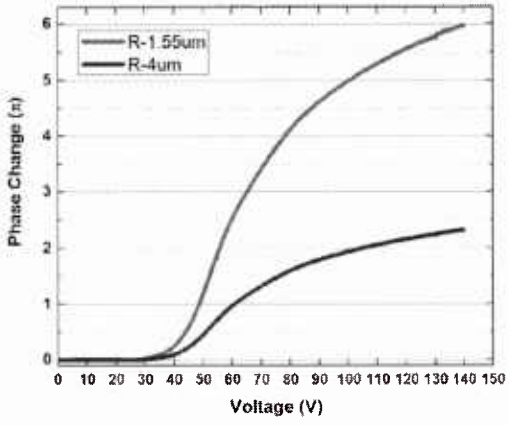

Fig. 10: Voltage-dependent phase change in a reflective mode PNLC at λ=1.5μm (measured) and λ=4μm (extrapolated).

To characterize the electro-optic properties of our PNLC cell, we measured its voltage-dependent transmittance (VT) curve with a laser beam at λ=1.55μm. Our ITO-glass substrate is not transparent at MWIR, so we converted the measured results at λ=1.55μm to λ=4μm. The PNLC cell was sandwiched between two crossed polarizers, with the rubbing direction at 45° to the polarizer's transmission axis. We converted the VT curve into voltage-dependent phase curve as depicted in Fig. 10. According to the dispersion curve shown in Fig. 7, the birefringence is insensitive to the wavelength in the MWIR region. Therefore, based on Eq. (4), we can transfer the voltage-dependent phase change curve from 1.55μm to 4μm easily. Thus, the operation voltage ($V_{2\pi}$) is 105V at λ=4μm. Such a high operation voltage of PNLC is due to the strong anchoring force provided by the polymer network.

However, it is the polymer network that helps decrease the response time. Figure 11 shows the measured decay time of the PNLC cell. The initial biased voltage is 105V. Similar to measuring free relaxation time, the biased voltage was removed spontaneously at t=0. Thus, the decay process initiated from 2π phase change at λ=4μm was recorded. If we count the phase decay time from 100% to 10%, it is only 3.6ms, which is ~42X faster than the traditional nematic LC mentioned previously.

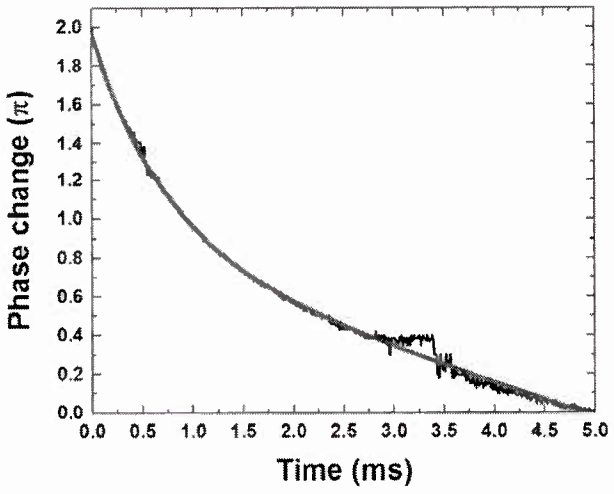

Fig. 11: Measured phase decay time of the PNLC sample. Black line is experimental data and red line is fitting with Eq. (7) and $\varphi_0 = 2\pi$.

4. Future work

4.1. MWIR

More chlorinated compounds will be developed with nematic phase and low absorption coefficient in the MWIR region. Besides, we will mix more LC compounds into eutectic mixture to decrease the melting point below room temperature, while maintaining low absorption, high birefringence, and modest dielectric anisotropy. When the mixture is ready, we plan to deliver our low-loss and high Δn LC mixture to Vescent Photonics or Raytheon for device testing.

4.2. LWIR

The =C-H in-plane deformation in the phenyl ring is the main cause for strong absorption near 10.6 μm. *Deuteration in the phenyl ring only* should shift this absorption band toward the longer wavelength side, which is outside the LWIR region. [S.T. Wu et al, J. Appl. Phys. 92, 7146 (2002)] From Table 1, the -C-H deformations in alkyl chain occur around 1430-1485 cm^{-1}. Deuteration on alkyl chain may shift this band to 1000 cm^{-1}, which is undesirable. Therefore, we propose to synthesize the LC compounds with deuteration or chlorination only in the phenyl rings as shown in the following:

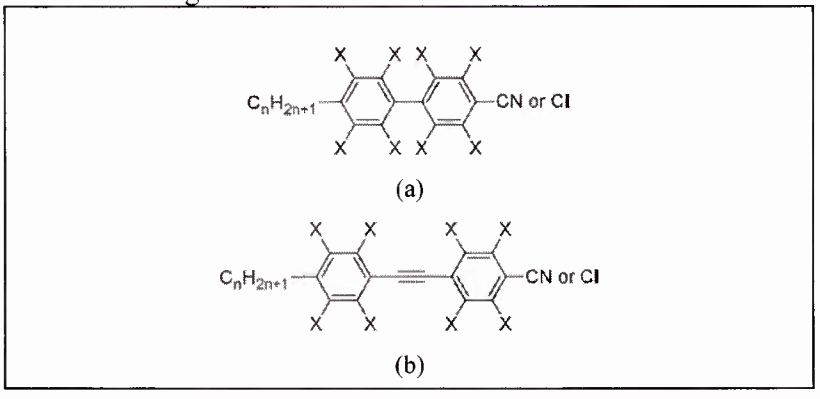

Fig. 14: Proposed low absorption compounds for LWIR, X=D or Cl.

4.3. SWIR

Liquid crystals with low absorption in MWIR usually exhibit low absorption in SWIR, since the absorption in SWIR results from the overtone or combination of the absorption in MWIR. This concept has been proven by comparing the absorption of 5CB and D5CB in SWIR region [ST Wu, et al. J. Appl. Phys. 92, 7146 (2002)]. We also plan to measure the absorption of our low-loss LC mixture designed for MWIR in the SWIR region.